Weather Effects on Obstacle Detection for Autonomous Car

Rui Song[1][a], Jon Wetherall[2][b], Simon Maskell[1][c] and Jason F. Ralph[1][d]
[1]*Dept. Electrical Engineering and Electronics University of Liverpool Liverpool, U.K.*
[2]*CGA Simulation, Liverpool, U.K.*

Keywords: Autonomous Vehicle, Multiple Sensors, Weather Simulation, Virtual Environment, Object Detection.

Abstract: Adverse weather conditions have become a critical issue when developing autonomous vehicles and driver assistance systems. Training and testing autonomous vehicles in a simulation environment before deploying them into the market have many benefits due to lower costs and fewer risks. However, there are only a few works about weather influences on sensors in the simulated environment. A more systematic study of weather effects on the sensors used on autonomous cars is required. This paper presents a multi-sensor simulation environment under different weather conditions and examines the influence on environmental perception and obstacle detection for autonomous cars. The simulation system is being developed as part of a collaborative project entitled: Artificial Learning Environment for Autonomous Driving (ALEAD). The system incorporates a suite of sensors typically used for autonomous cars. Each sensor model has been developed to be as realistic as possible – incorporating physical defects and other artefacts found in real sensors. The influence of weather on these sensors has been simulated based on experimental data. The multi-sensor system has been tested under different simulated weather conditions and analysed to determine the effect on detection of a dynamic obstacle and a road lane in a 3D environment.

1 INTRODUCTION

In recent years, there has been a significant move towards the development of semi-autonomous and fully autonomous vehicles. Autonomous transport offers increased convenience and an improved quality of life. It could help elderly and physically disabled people to have independence. Autonomous cars could reduce CO_2 emissions and lead to a revolution in urban transportation; less traffic congestion and lower transportation costs (in fuel and for infrastructure). According to the definition used by the Society of Automotive Engineers (SAE), the maximum autonomy level of autonomous vehicle is currently at level 3 out of 6 levels (Badue et al., 2019) – autonomous driving is possible under the supervision of an operator. The main reason for this limit is because of the difficulty in detecting and dealing with unexpected events, particularly when sensor performance is degraded due to environmental effects (weather, dirt, and possible damage). Such unexpected events could even lead to fatal crash (Nyholm, 2018). A close relation exists between autonomous driving and weather recognition, since in adverse weather conditions such as rain, fog, or snow, driving is more difficult than during fair conditions. The ability to tackle real life problems is critical to improve the autonomy level of cars and to reduce accidents. Because of the costs and risks associated with road trials, the trend is to train algorithms using simulations before putting autonomous cars into service on the road.

The demand for realistic simulation environments and recent advances in computer technology has led to significant improvements in simulation systems for autonomous cars. In traditional self-driving software, sensor data collected from real world are imported to test the reaction of the vehicle's control software to environmental changes, for example using recorded video streams to avoid other cars and pedestrians on

[a] https://orcid.org/0000-0002-8695-1522
[b] https://orcid.org/0000-0001-8477-9071
[c] https://orcid.org/0000-0003-1917-2913
[d] https://orcid.org/0000-0002-4946-9948

Song, R., Wetherall, J., Maskell, S. and Ralph, J.
Weather Effects on Obstacle Detection for Autonomous Car.
DOI: 10.5220/0009354503310341
In *Proceedings of the 6th International Conference on Vehicle Technology and Intelligent Transport Systems (VEHITS 2020)*, pages 331-341
ISBN: 978-989-758-419-0

road (Ess et al., 2009; Xu et al., 2017). To improve the stability and robustness of self-driving software, road networks, other vehicles, bicycles, pedestrians and even animals need to be included in the simulation (Tideman and van Noort 2013; Kehrer et al., 2018). In this way, developers can use virtual worlds to test and retest a variety. of scenarios found in everyday life and identify potential problem cases. Recently, sensor models, advanced visual perception and intelligent guidance systems have been integrated into simulation systems for sensing the vehicle's surroundings and to help avoid collisions.

Cameras and LiDAR are the two most popular sensors in visual navigation and car localization (Miklic et al., 2012; Shimchik et al., 2016; Häne et al., 2017). Radar simulation is gaining attention due to its robustness in most adverse weather conditions (Apollo, 2019; RFpro, 2019). One common problem with these simulated systems is that they are not suitable for real-time tests, especially when the 3D environment is complex. To solve the real-time problem, LGSVL combines the real world video data and the simulated sensing data together to train autonomous cars (LGSVL Simulator, 2019). VIRES Virtual Test Drive (VTD) improves the simulation environment that can be adjusted to different weather conditions (VIRES, 2019).

However, current systems do not generally provide models for the influence of weather on the sensors used on autonomous vehicles. As in human vision, these sensors are negatively impacted by adverse weather conditions. For example, rainy and foggy conditions cause significant degradation to the functions of camera and LiDAR (Dannheim et al., 2014), significantly reducing operating range and signal contrast. Therefore, accurate simulations of sensor performance in adverse weather conditions are particularly important for the further development of simulation software for autonomous vehicles.

Based on the multi-sensor system developed for the Artificial Learning Environment for Autonomous Driving (ALEAD) project (Song et al.,2019), shown in Figure 1, a range of different weather effects on onboard sensors have been simulated in this paper. To investigate the influence of these effects on autonomous vehicle navigation, a scene with a ball bouncing in a street has been simulated in Unity3D. A tracking algorithm has been developed and implemented to detect the movement of the bouncing ball and to separate it from the surrounding clutter. The paper is organized as follows. Section 2 details the ALEAD project and the multi-sensor system. Section 3 and 4 explain the methods used in weather simulation and object detection, respectively. Results are shown and discussed in Section 5. The paper is summarized, and conclusions drawn in Section 6.

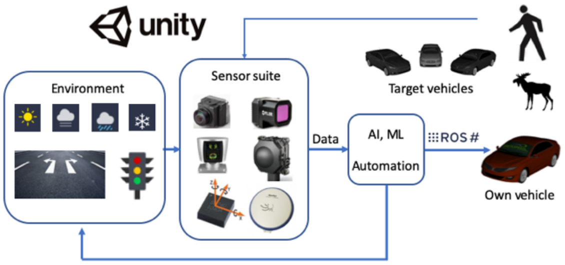

Figure 1: Structure of ALEAD simulator.

2 ALEAD PROJECT

2.1 Project Overview

ALEAD is a digital environment that provides autonomous vehicles a virtual space to learn to drive and to respond to external stimuli, thereby reducing costs and time associated with road tests[1]. ALEAD is being based around industry standard software components. As shown in Figure 1, most simulations are run in the Unity3D graphics engine, and is interfacing with the Robot Operating System (ROS) and autonomous car models, including the Baidu Apollo (Apollo, 2019) open driving solution.

Existing computer game simulation technologies developed by the industrial partner CGA are being applied to autonomous vehicle training, using novel improvements to existing simulation systems and applying these systems in a new sector. By using artificial intelligence (AI) and machine learning (ML) to train vehicles in an extensive simulated world, designed with real world inputs and benefiting from the integration of multiple sensors, ALEAD is combining technologies to create a wholly new environment which could have a significant impact on the time required to get autonomous vehicles on the road. ALEAD focuses on the merging fields of machine learning, virtual reality, augmented reality in realistic simulations of urban environments.

The ALEAD project will significantly reduce the need for live trials of autonomous vehicles. Using a

[1] ALEAD is capable of doing online testing, but also rerun problematic cases (using stored random number seeds) and run at less than real-time (e.g. to facilitate testing of new algorithms). It can give control of time to the user and generate multiple images simultaneously.

large number of parallel simulated environments, it will be possible to train systems much faster than running live trials and across a range of exceptional weather conditions, such as fog or ice.

2.2 Sensor Suite

Current testing systems mainly use video information and live trials. The key to simulating the environment in as realistic way as possible is the use of physically realistic sensor models and environmental factors. This contrasts with work to accurately model the physics of the sensor platform (Which has been the focus of the development of VTD). The ALEAD system is developing a representative sensor suite including models for each of the key sensors that are likely to be present in future autonomous vehicles, including short range Radar, IR cameras, LiDAR scanners, and GPS. The aim is to identify the factors that determine or limit sensor performance, thereby having an adverse effect on the robustness and safety of an autonomous vehicle: including, precipitation and other atmospheric effects, such as high humidity or fog, bright sources of illumination, such as the sun being low in the sky and reflections from buildings, erratic behavior from other road users, debris in the road, and deliberate jamming of the sensor data. The sensor modelling will make the training physically realistic for computer vision, which operates very differently from human perception.

2.2.1 Image

A standard visible band camera model uses the simple scene as a basis. The angle of the field of view (FOV) will be defined based on the interface with the coverage of other sensors. In this paper, the camera sensor is used directly from the original camera of Unity3D. To accelerate processing, only objects near the camera are rendered. The output of the camera only includes these rendered objects and objects out of range are ignored. The FOV of the camera is set as 38^o, and a perspective projection is used.

Infrared Band camera generates thermal images of the scene are based on the three-dimensional geometry of the scene and require objects within the scene to be labelled with temperature information. Also requires some indication of the atmospheric properties to derive path radiance and attenuation properties. The infrared scene shares the same 3D scene rendered for the visible band camera, since the physical objects are the same in each case. Moreover, the infrared scene includes a temperature map, where temperature profiles to different surfaces present in the visible band scene are allocated. The IR camera model utilizes this temperature map and converts the temperatures into thermal intensities/photon fluxes (Griffith et al., 2018). The thermal radiation is propagated through an atmospheric model (including attenuation and path radiance) and then detected using a bespoke infrared camera model with properties representative of a commercial infrared camera (pixel non-uniformities, limited pixel resolution, dead/saturated pixels, etc.) (Ahire, 2014). The FOV of IR camera is set as 59^o, with limited resolution to reflect the smaller focal plane arrays typically available in infrared cameras.

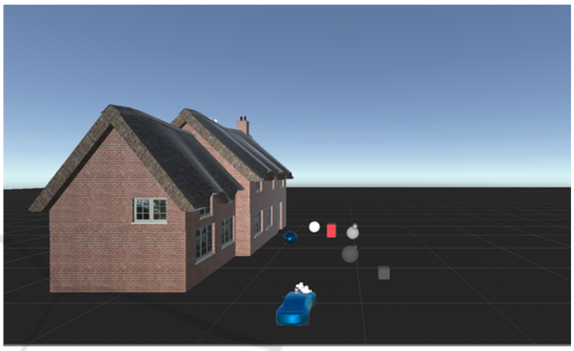

Figure 2: A simple constructed scene.

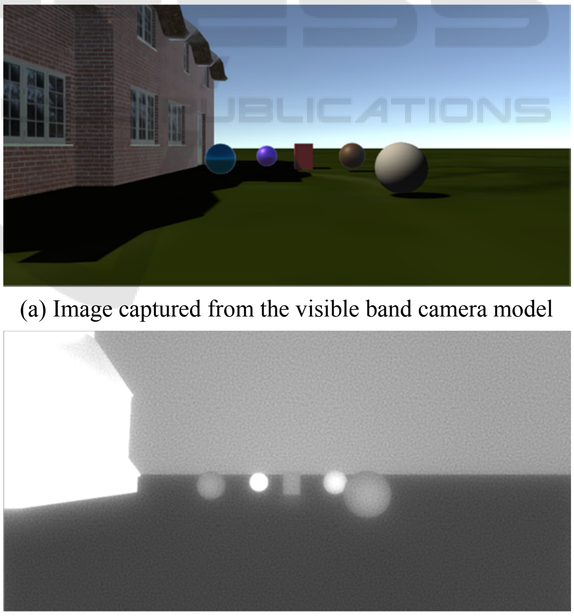

(a) Image captured from the visible band camera model

(b) Image captured from the simulated IR camera

Figure 3: Rendering results from imaging sensors.

To test the functionality of simulated sensors, a simple scene shown in Figure 2 has created with a cottage and several sphere and cubic objects around an autonomous car. The cameras are mounted behind the windshield of the autonomous car to get realistic data in the rain. The position of the IR camera is set beside the camera. The rendering results from camera and IR camera are shown in Figure 3(a) and (b), respectively.

2.2.2 LiDAR

LiDAR is an active near visible band sensor (Near Infrared Band), which measures the time of flight of pulsed light to build up a three-dimensional map of the scene. The scanning processes will be presented while vehicle is in motion and reflection of light from the surfaces of objects in the scene.

A commercial LiDAR sensor is simulated to ensure that the representation is as realistic as possible. The Velodyne HDL-64E (Velodyne Manual, 2014), a vertical LiDAR sensor is used because it is the most popular type used in self-driving cars ((Bergelt et al., 2017). To simulate this type of LiDAR sensor, parameters such as the number of lasers, position of each individual laser and its angle, and the rotational speed have been included in the model.

In Unity3D, each laser can be represented using ray-casting. From a mathematical perspective, ray-casting is a directional 3D vector, which checks for intersections with other geometries. The coordinate of the intersected point will be sent back. In such a way, the ray-casting can be considered to be a realistic representation of a laser scanner. Note that this requires the creation of a collider for each object built in the constructed scene. Unity3D uses the physics engine to handle ray-casting. Multiple ray-casts can be executed within a single physics frame. In this way, it can provide simultaneous actions. Figure. 4 shows the result of a 360° LiDAR scanning in the scene.

2.2.3 Radar

Radar is a simple distance measuring device with relatively broad beam width and short range – but with better bad weather performance than LiDAR or cameras. Usually, in the driving environment, the radar cross section (RCS) of obstacles is relatively small. Therefore, the type of radar used in an autonomous car is a broadband Frequency Modulated Continuous Wave (FMCW) radar (Belfiore et al., 2017). It detects multiple objects and their respective distances by performing a fast Fourier transform (FFT) on the interference beat-frequency signal.

Figure 4 illustrates the radar sensing result. In the scene, each object has a defined radar signature with RCS information (green circles). Ray-casts (green lines) are used to represent radar beams. It can be seen that the cubic object, pointed by a red arrow is not detected by the radar as it is out of the detection range.

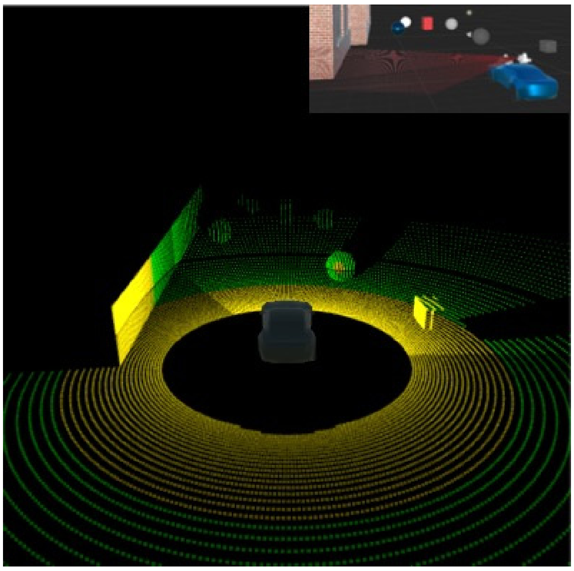

Figure 4: LiDAR sensing result with a scanning of 360° in the simple constructed scene. Laser beams are represented by red lines.

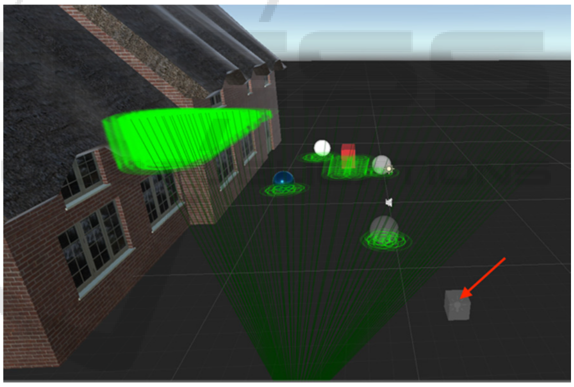

Figure 5: Radar using ray-casting, with detection of RCS.

2.2.4 GPS

GPS/GNSS Satellite Navigation Systems use basic radio navigation based on very low power satellite signals, and it requires WGS’84 Earth model information for realistic satellite data, including an interface for live GPS/GNSS feed or recorded satellite ephemeris data (e.g. RINEX format). The position of the vehicle, in terms of longitude, latitude and altitude, is calculated using the distance between the vehicle and the satellites within view. To get an accurate position, at least 4 satellites should be visible, although often six to eight may actually be visible. The total number of satellites is 32.

3 WEATHER EFFECTS ON SENSORS

From the investigations of (Rasshofer and Gresser, 2005), the influence of weather on sensors can be summarized as shown in Figure 6. It can be seen that image sensors, camera and IR camera, and LiDAR are most prone to be influenced in rainy and foggy weather. Therefore, this paper focuses on simulation of these sensing technologies for autonomous vehicles and their respective issues under adverse weather conditions of rain and fog.

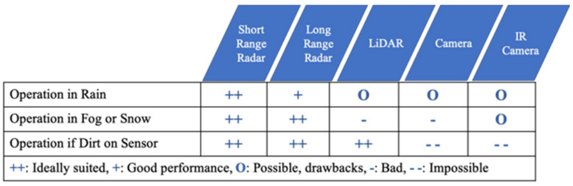

	Short Range Radar	Long Range Radar	LiDAR	Camera	IR Camera
Operation in Rain	++	+	O	O	O
Operation in Fog or Snow	++	++	-	-	O
Operation if Dirt on Sensor	++	++	++	- -	- -

++: Ideally suited, +: Good performance, O: Possible, drawbacks, -: Bad, - -: Impossible

Figure 6: Typical strengths and weaknesses of automotive sensors in different weather environments.

3.1 Rainy Conditions

In Unity3D, rain is simulated using a particle-based system, where the intensity of rain can be adjusted. The shape of droplet spread on the windshield is assumed to be an ellipse.

3.1.1 Camera and IR camera

Rainy weather introduces sharp intensity fluctuations due to increased atmospheric scattering and general obscuration, which degrade the quality of images and videos taken from a standard camera (Garg and Nayar, 2005). IR cameras perform similarly in the presence of rain. Because both visible and IR cameras are set behind windshield, raindrops that stay on the glass can create a raindrop pattern on the image, which decreases the image intensity and blurs the edges of other patterns behind it (Bernard et al., 2014).

Figure 7 (a) and (b) show the results of images captured from the visible band and IR camera models, respectively under rainy weather. Comparing Figure 7 with Figure 3, it can be seen that the contrast of both the visible band and IR camera images have reduced slightly. The areas that have strong contrast in color and covered by raindrops are distorted with reflection of some patterns behind raindrops. Whereas those areas with less contrast were blurred.

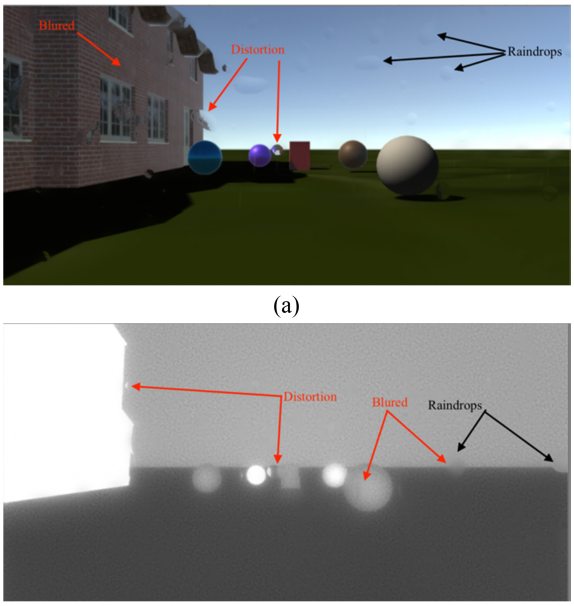

(a)

(b)

Figure 7: Results of captured images in rainy conditions. (a) Camera image, (b) IR camera image.

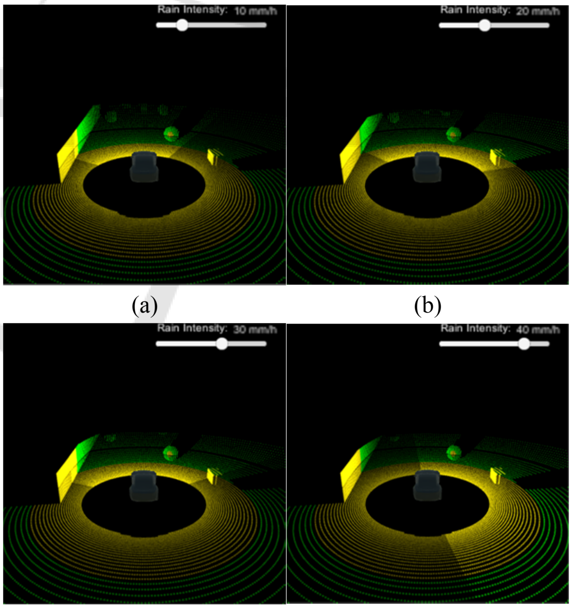

(a) (b)

(c) (d)

Figure 8: LiDAR scanning results in rainy conditions with different rate of rain. From (a) to (d), the rain rate increases from 10 mm/h to 40 mm/h.

3.1.2 LiDAR

There are several studies on laser pulse transmission through rain Rasshofer et al., 2011; Hasirlioglu et al., 2016; Filgueira et al., 2017). The relationship between rain rate and laser power is modeled by

(Goodin et al., 2019). In this paper, the detection range Z influenced by rain can be modeled using:

$$Z' = Z + 0.02Z(1-e^{-R})^2 \tag{1}$$

where Z' is the modified detection range affected by rain, and 0.02 is the variance factor. The rate of rain is denoted as R. Note that the sizes of the raindrops are assumed to be the same.

The scanning results from LiDAR model at different rain rates predicted by Equation (1) are shown in Figure 8. By comparing Figure 4 and Figure 8(a), it can be seen that the detected maximum distance of target is reduced. When the rain rate increases from 10 mm/h to 40 mm/h, the detection range decreases further, and the number of detected objects were reduced accordingly. Moreover, the shapes or outlines of some objects cannot be presented completely by point clouds.

3.2 Foggy Conditions

From the definition, fog can be considered to be microscopic water droplets. Therefore, the influence of fog on LiDAR scanning is similar to the effect of rain, as presented in Section 3.1.2, but the variance factor in Equation (1) changes to 0.17 (Heinzler et al., 2019).

When light passes through the atmosphere or liquid, it can be absorbed, scattered, and reflected anywhere in space without hitting a solid surface. As with rain, the scattering due to fog can lead to extinction of an optical signal. The relationship between visibility and the extinction coefficient due to fog can be expressed as:

$$V = \frac{ln(0.05)}{k} \approx \frac{3}{k} \tag{2}$$

where V is the distance that the value through fog is reduced to 5% of its original value. k is the extinction coefficient (Duthon et al., 2019).

The extinction coefficient also varies with wavelengths (Nebuloni, 2005). Table 1 below summaries the extinction coefficient (per km) value of different wavelengths with different visibility.

Table 1: Extinction coefficient values of different wavelengths (Nebuloni 2005).

Wavelength	Visibility V (km)	k
Visible	V>0	3.91
Near IR (Inc)	0.06 <V < 0.5	3.65
	0.5 < V < 2	2.85
IR	0.06 <V < 0.5	3.01
	0.5 <V <10	2.40

To simulate fog, an approximation method using exponential model is applied:

$$f = e^{-cd} \tag{3}$$

where c is the coordinate of fog (is where to render colour of fog), and d is the density of fog. After adopting the extinction coefficients for the visible band and IR camera into image rendering, the results are shown in Figure 9 and Figure 10, respectively. As shown in Figure 9(a) and (b), when the density of fog increases from 0.4 to 0.8 (fog density varies between 0 to 1), the spherical object indicated by the red arrow can hardly be seen due to the longer distance. However, comparing to IR camera results, the intensity reduction is less and the spherical object can still be seen. When the car moves closer to objects in the scene, those objects initially at longer distances can be seen clearly.

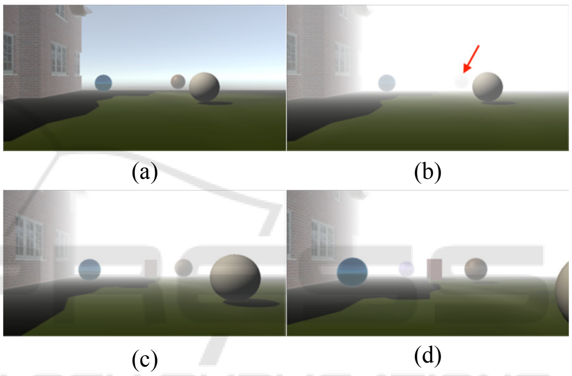

Figure 9: Image results from camera in foggy conditions. (a) Fog density=0.4, (b) fog density=0.8, (c) and (d) same fog density, but camera moves forward.

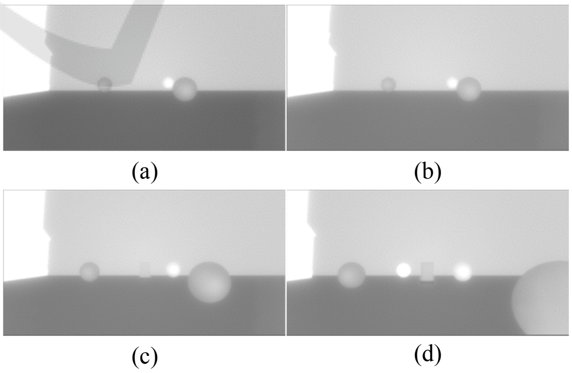

Figure 10: Image results from IR camera in foggy conditions. (a) fog density=0.4, (b) fog density = 0.8, (c) and (d) same fog density, but IR camera moves forward.

4 OBJECT DETECTION

After understanding how weather affects sensor data, the next task is to investigate how autonomous driving and navigation will be affected. A more complex scene shown in Figure 11 was created, consisting of a road network, vegetation and houses. The models of sensors and weather effects simulated in Section 3 are integrated into the scene to allow the autonomous car detecting and tracking objects while driving. The data received from sensors are presented in a display window (Figure 12), where the left represents point clouds generated by LiDAR data and GPS information is displayed at the top left corner. The right side shows the rendering images from IR camera and visible band camera, respectively. Radar beams are plotted as green lines in the camera image.

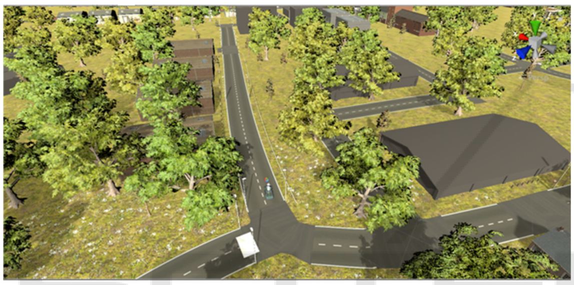

Figure 11: Complex scene. Road network, including road marks, buildings and vegetation are simulated.

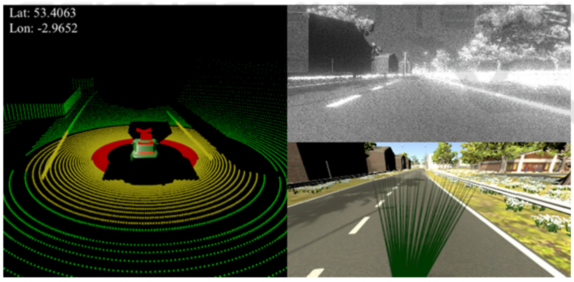

Figure 12: Display window of multi-sensor results.

In this paper, the weather influences on object detection are considered. Two simulation scenarios are proposed:

- Scenario 1: detection of road lanes while driving;
- Scenario 2: detection of a ball bouncing in the street.

Video streams recorded from the cameras are selected as data for detection. Rain is added, as an example of adverse weather effect, in both scenarios. The main methodologies used for detections in these two scenarios are Hough transformation (Duda and Hart, 1972) and Background difference method (Philip, 2013), respectively.

4.1 Road Lane Detection

A flow chart of the procedures to detect road lanes using Hough transformation is shown in Figure 13. Firstly, the rendered image from the camera is converted into a 'birds-eye view' image. A Sobel operator is applied to calculate thresholds of gradient and color that represented by hue, saturation and lightness (HSL) values. The lane line on both side of car can be extracted thereafter. Then, the curve of each line is fitted using sliding window technique to derive the corresponding second degree polynomial function. In such a way, the positions of pixel points of lines can be obtained. The last step is to warp the 'birds-eye view' back to camera view with lines projected.

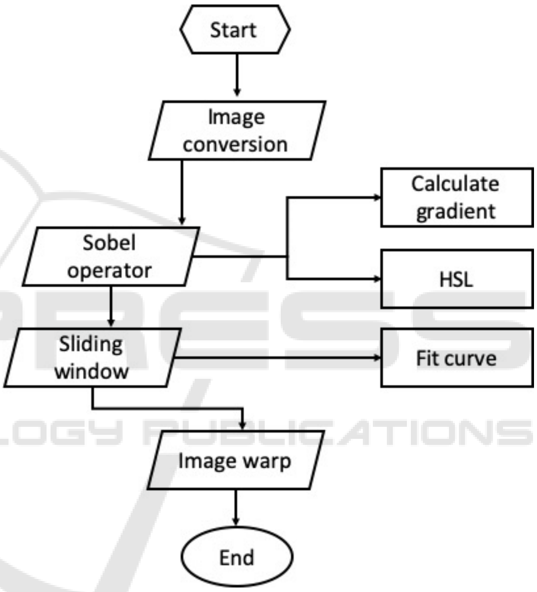

Figure 13: Flow chart of Hough transformation.

4.2 Ball Detection

In Scenario 2, it is assumed that the bouncing ball is the only dynamic obstacle in the scene, whereas the car is not moving (for simplicity). The background difference method is usually used where a scene is relatively static – the stationary constraint for the car can be relaxed by aligning the background between frames using image registration, but this is not considered here.

In the background difference method, a background frame is selected first by taking an average over a certain number of frames. In such a way, the slow motion of raindrops can be neglected. Then, a grayscale subtraction operation is performed on the current frame image and the background image, and the absolute values are taken. The values are compared with a threshold value to generate foreground pixels (values greater than the threshold). Foreground pixels are determined thereafter. The center of the ball can be calculated by enlarging the foreground pixels.

5 RESULTS

5.1 Scenario 1

In Scenario 1, two simulations (Simulation 1.1 and 1.2) are tested. The car is set to start at the same location and drive along the same road. Simulation 1.1 is driven in clear sky environment, while Simulation 1.2 is driven in rainy weather. The results for road lane detection are shown in Figure 14 and 15, respectively. The lane region is coloured in green, with the outline plotted in red/yellow.

It can be seen from Figure 14 that road lanes can be detected successfully, but with slight offsets at the bottom of Figures 14(a) and (b). This is because the lane color vanishes which leads to lower contrast. However, in rainy conditions, offsets increase due to distortions of the road lanes. Comparing Figure 15(a) to (c), it can be seen that when the number of distortion areas increases (more rain drops), offsets increase as well. Moreover, in Figure 15(d), only the road lane on the right side of car is segmented.

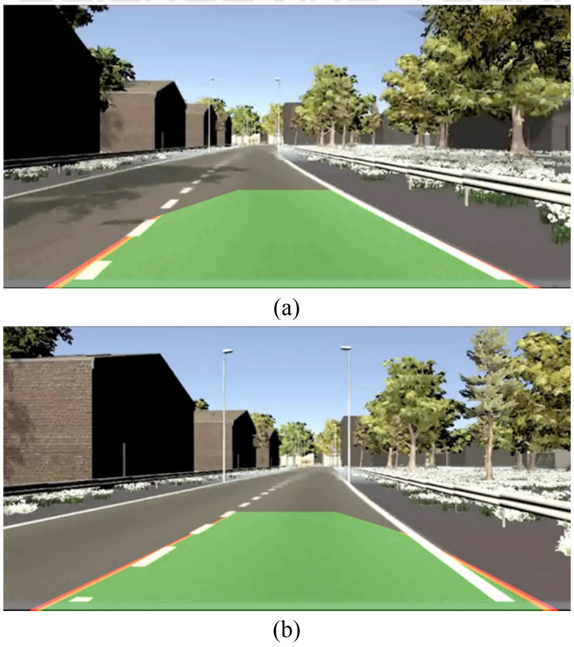

(a)

(b)

Figure 14: Road lane detection in clear sky. (a) and (b) are the car driving at different time steps.

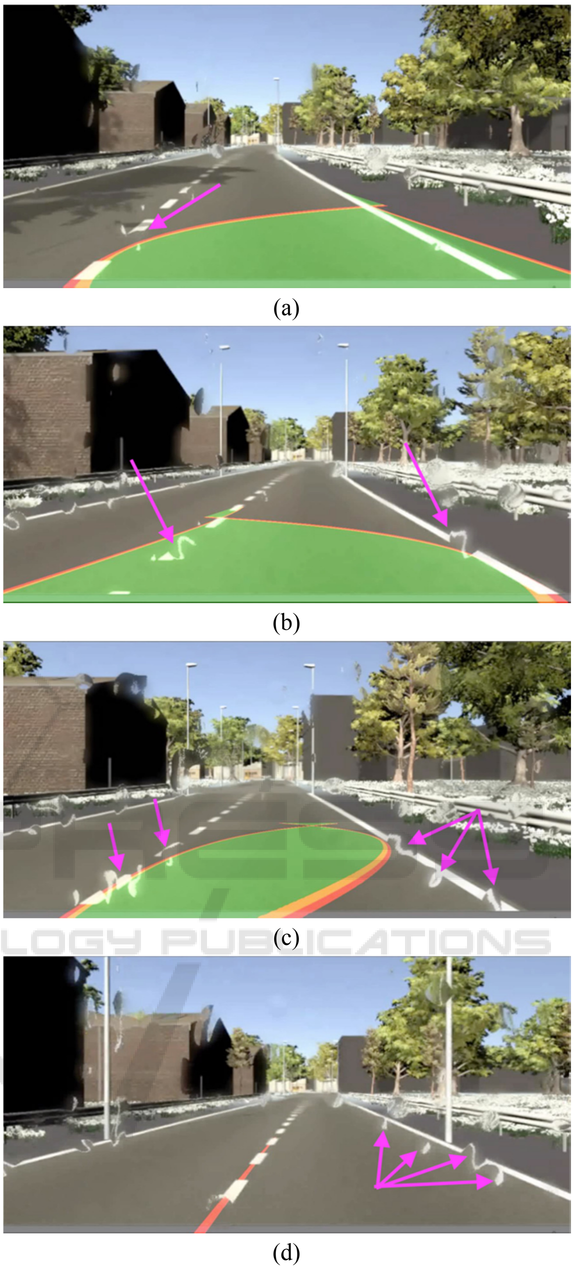

(a)

(b)

(c)

(d)

Figure 15: Road lane detection in rainy conditions. (a) to (d) are the car driving at different time steps.

5.2 Scenario 2

In Scenario 2, two simulations (Simulation 2.1 and 2.2) are tested in clear sky and rainy conditions, respectively. The results for detecting the bouncing ball in these two simulations are presented in Figure 16 to 20 at different time steps. The centres of the detected ball positions are marked using green boxes.

All segmentations of the ball in Simulation 2.1 are successful. For Simulation 2.2, the ball can be detected if the ball is not covered by raindrops, as shown in Figure 16(b) and Figure 17(b). When the ball is partly covered by raindrops (Figure 19b) or near a raindrop (Figure 20b), the ball can still be detected, but the center will be shifted. Whereas, when the ball is fully covered by raindrops, it cannot be detected at all. In this case, a red box is plotted in the middle of the image, as shown in Figure 18(b).

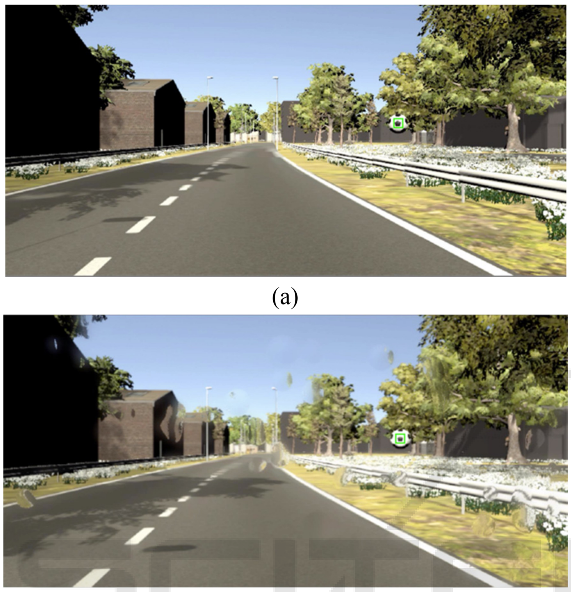
(a)

(b)

Figure 16: Ball detection at time step 1. (a) Simulation 2.1, (b) Simulation 2.2.

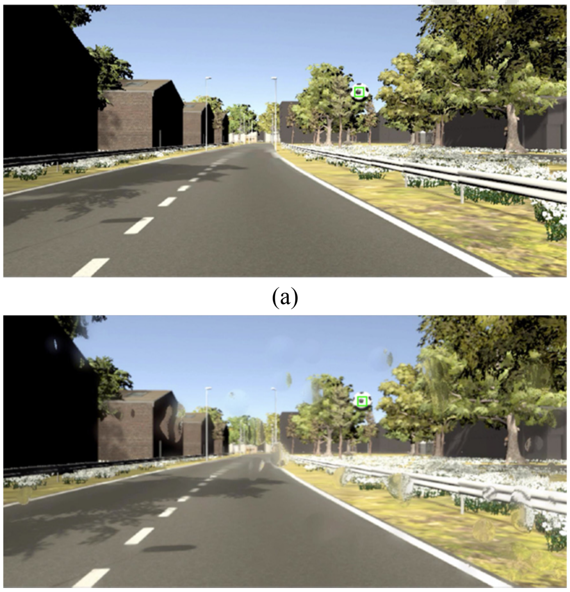
(a)

(b)

Figure 17: Ball detection at time step 30. (a) Simulation 2.1, (b) Simulation 2.2.

The detected positions of the bouncing ball are plotted in Figure 21. The results of Simulation 2.1 and 2.2 are presented in red and blue color, respectively. It can be investigated that there are offsets between red and blue plots. The main reason is because of the noise generated by raindrops.

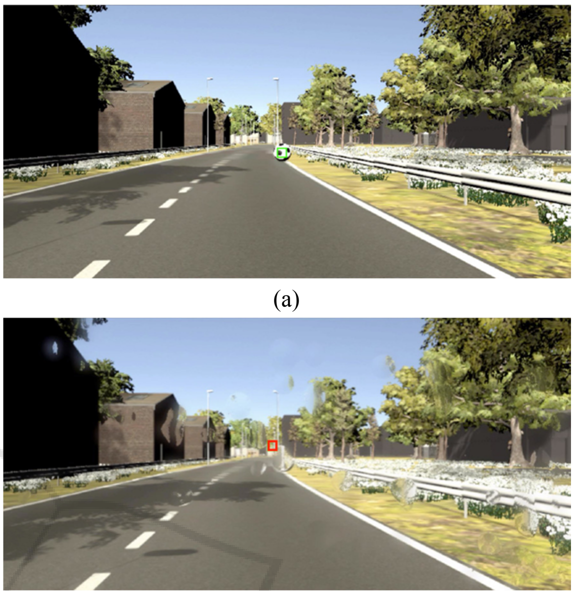
(a)

(b)

Figure 18: Ball detection at time step 100. (a) Simulation 2.1, (b) Simulation 2.2.

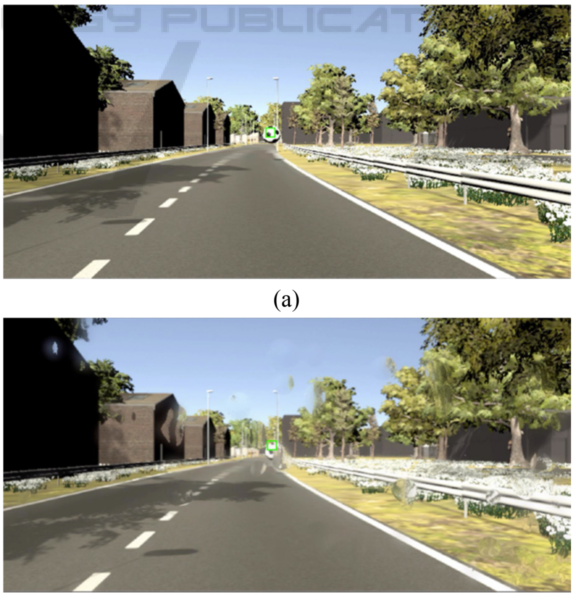
(a)

(b)

Figure 19: Ball detection at time step 110. (a) Simulation 2.1, (b) Simulation 2.2.

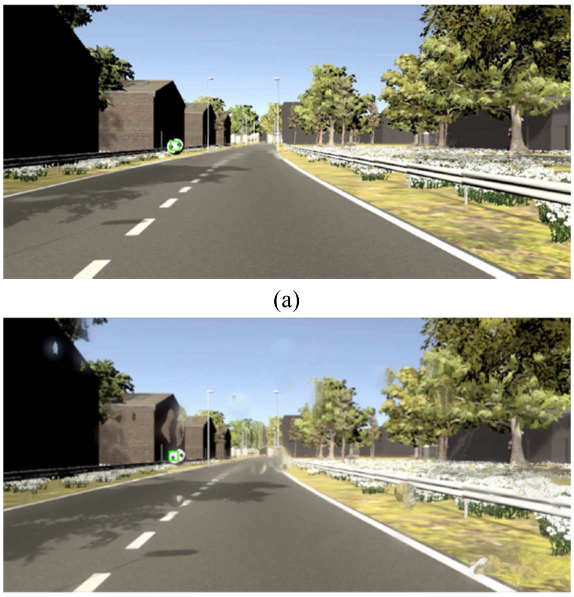

(a)

(b)

Figure 20: Ball detection at time step 180. (a) Simulation 2.1, (b) Simulation 2.2.

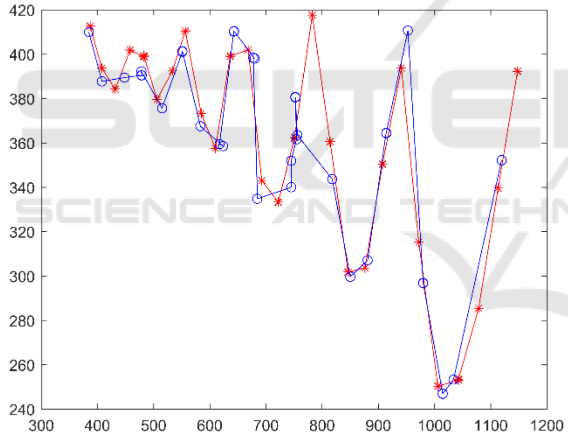

Figure 21: Detected positions of the bouncing ball. Results of Simulation 2.1 and 2.2 in clear sky and rainy weather are presented in red and blue colour, respectively.

6 CONCLUSIONS

In this paper, a multi-sensor system has been developed for the ALEAD project allowing autonomous car models to perceive surrounding environment in simulated scenes. The influence of weather on the sensing data for each of the sensors has been implemented to make the simulation as close to a realistic environment as possible. Image processing methods have been applied to detect road lanes and a moving obstacle in rainy conditions. Simulation results show that adverse weather can have a significant effect on lane following and object detection. In the case of moving object detection, the ability to track and evade moving obstacles may deteriorate significantly in rainy conditions.

For future work, more advanced segmentation algorithms, such as deep learning methods, will be applied to improve the accuracy of object detection and tracking. Edge case usages for the sensors will be simulated to enhance the realism and to explore the 'worst case' scenarios that are possible for autonomous vehicles, for example, various light conditions and sever rain, and to investigate the response of automated driving systems in such cases.

ACKNOWLEDGEMENTS

This is a collaborative work between University of Liverpool and CGA Simulation as part of the Connected and Autonomous Vehicle programme. It is funded by the Innovate UK, with Grant No. 104274. The authors are also indebted to Mr. Dave Griffiths and Mr Ben Mitchell for their work on making the animations in the 3D scene and creating the temperature map. Thanks to the feedback received from Daimler on our previous work, and this paper is a partial response to it.

REFERENCES

Ahire, A. S. (2014). Night vision system in BMW. *International Review of Applied Engineering Research*, *4*(1), 1-10.

Apollo. (2019). Apollo [online].

Badue, C., Guidolini, R., Carneiro, R. V., Azevedo, P., Cardoso, V. B., Forechi, A., ... & Oliveira-Santos, T. (2019). Self-driving cars: A survey. *arXiv preprint arXiv:1901.04407*.

Belfiore, F., Calcagno, A., Borgonovo, G., Castro, M. G., Pisasale, A., Platania, M., ... & Salomon, A. M. (2017, October). A 76 to 81GHz packaged transceiver for automotive radar with FMCW modulator and ADC. In *2017 European Radar Conference (EURAD)* (pp. 143-146). IEEE.

Bergelt, R., Khan, O., & Hardt, W. (2017). Improving the intrinsic calibration of a velodyne lidar sensor. In *2017 IEEE SENSORS* (pp. 1-3). IEEE.

Bernard, E., N. Rivière, M. Renaudat, M. Péalat and E. Zenou (2014). Active and thermal imaging performance under bad weather conditions. France, Europe.

Dannheim, C., Icking, C., Mäder, M., & Sallis, P. (2014, May). Weather detection in vehicles by means of camera and LIDAR systems. In *2014 Sixth International Conference on Computational Intelligence, Communication Systems and Networks* (pp. 186-191). IEEE.

Duda, R. O., & Hart, P. E. (1971). *Use of the Hough transformation to detect lines and curves in pictures* (No. SRI-TN-36). Sri International Menlo Park Ca Artificial Intelligence Center.

Duthon, P., Colomb, M., & Bernardin, F. (2019). Light transmission in fog: The influence of wavelength on the extinction coefficient. *Applied Sciences*, *9*(14), 2843.

Ess, A., Leibe, B., Schindler, K., & Van Gool, L. (2009, May). Moving obstacle detection in highly dynamic scenes. In *2009 IEEE International Conference on Robotics and Automation* (pp. 56-63). IEEE.

Filgueira, A., González-Jorge, H., Lagüela, S., Díaz-Vilariño, L., & Arias, P. (2017). Quantifying the influence of rain in LiDAR performance. *Measurement*, *95*, 143-148.

Garg, K., & Nayar, S. K. (2005, October). When does a camera see rain? In *Tenth IEEE International Conference on Computer Vision (ICCV'05) Volume 1* (Vol. 2, pp. 1067-1074). IEEE.

Goodin, C., Carruth, D., Doude, M., & Hudson, C. (2019). Predicting the Influence of Rain on LIDAR in ADAS. *Electronics*, *8*(1), 89.

Griffith, E. J., Mishra, C., Ralph, J. F., & Maskell, S. (2018). A system for the generation of synthetic Wide Area Aerial surveillance imagery. *Simulation Modelling Practice and Theory*, *84*, 286-308.

Häne, C., Heng, L., Lee, G. H., Fraundorfer, F., Furgale, P., Sattler, T., & Pollefeys, M. (2017). 3D visual perception for self-driving cars using a multi-camera system: Calibration, mapping, localization, and obstacle detection. *Image and Vision Computing*, *68*, 14-27.

Hasirlioglu, S., Doric, I., Lauerer, C., & Brandmeier, T. (2016, June). Modeling and simulation of rain for the test of automotive sensor systems. In *2016 IEEE Intelligent Vehicles Symposium (IV)* (pp. 286-291). IEEE.

Heinzler, R., Schindler, P., Seekircher, J., Ritter, W., & Stork, W. (2019). Weather Influence and Classification with Automotive Lidar Sensors. *arXiv preprint arXiv:1906.07675*.

Kehrer, M., Pitz, J., Rothermel, T., & Reuss, H. C. (2018). Framework for interactive testing and development of highly automated driving functions. In *18. Internationales Stuttgarter Symposium* (pp. 659-669). Springer Vieweg, Wiesbaden.

LGSVL Simulator (2019). LGSVL Simulator: An Autonomous Vehicle Simulator [Online].

Miklić, D., Petrović, T., Čorić, M., Pišković, Z., & Bogdan, S. (2012, May). A modular control system for warehouse automation-algorithms and simulations in USARSim. In *2012 IEEE International Conference on Robotics and Automation* (pp. 3449-3454). IEEE.

Nebuloni, R. (2005). Empirical relationships between extinction coefficient and visibility in fog. *Applied optics*, *44*(18), 3795-3804.

Nyholm, S. (2018). The ethics of crashes with self□driving cars: A roadmap, II. *Philosophy Compass*, *13*(7), e12506.

Philip, A. S. (2013). Background subtraction algorithm for moving object detection using denoising architecture in FPGA. *Int. J. Sci. Res*, *2*, 151-157.

Rasshofer, R. H., & Gresser, K. (2005). Automotive radar and lidar systems for next generation driver assistance functions. *Advances in Radio Science*, *3*(B. 4), 205-209.

Rasshofer, R. H., Spies, M., & Spies, H. (2011). Influences of weather phenomena on automotive laser radar systems. *Advances in Radio Science*, *9*(B. 2), 49-60.

RFpro. (2019). Driving Simulation | Deep Learning Automated Driving | Vehicle Dynamics [Online].

Shimchik, I., Sagitov, A., Afanasyev, I., Matsuno, F., & Magid, E. (2016). Golf cart prototype development and navigation simulation using ROS and Gazebo. In *MATEC Web of Conferences* (Vol. 75, p. 09005).

EDP Sciences.

Song, R., Wetherall, J., Maskell, S., & Ralph, J.F. (2019). A Multi-Sensor Simulation Environment for Autonomous Cars. In 2019 22nd International Conference on Information Fusion (FUSION) (pp.). IEEE.

Tideman, M., & Van Noort, M. (2013, June). A simulation tool suite for developing connected vehicle systems. In *2013 IEEE Intelligent Vehicles Symposium (IV)* (pp. 713-718). IEEE.

Velodyne Manual (2014). High Definition LiDAR - HDL 64E User Manual [Online].

VIRES (2019). VTD—virtual test drive [Online].

Xu, H., Gao, Y., Yu, F., & Darrell, T. (2017). End-to-end learning of driving models from large-scale video datasets. In *Proceedings of the IEEE conference on computer vision and pattern recognition* (pp. 2174-2182).